

ADVANCED MATERIALS

Supporting Information

for *Adv. Mater.*, DOI: 10.1002/adma.201502814

Single Cell Nanobiosensors for Dynamic Gene Expression
Profiling in Native Tissue Microenvironments

*Shue Wang, Reza Riahi, Na Li, Donna D. Zhang, and Pak Kin
Wong**

Supporting Information

Single Cell Nanobiosensors for Dynamic Gene Expression Profiling in Native Tissue Microenvironments

By *Shue Wang, Reza Riahi, Na. Li, Donna D. Zhang, and Pak Kin Wong**

S. Wang and Prof. P. K. Wong
Department of Aerospace and Mechanical Engineering
The University of Arizona
Tucson, AZ, 85721, USA
E-mail: pak@email.arizona.edu

Prof. P. K. Wong
Department of Biomedical Engineering and Department of Mechanical and Nuclear Engineering
The Pennsylvania State University
University Park, PA, 16802

R. Riahi
Harvard-MIT Health Sciences and Technology
Massachusetts Institute of Technology and Harvard Medical School
Cambridge, MA 02139, USA

Prof. N. Li
Department of Mechanical and Aerospace Engineering
University of Miami
Coral Gables, FL 33146, USA

Prof. D. D. Zhang
Department of Pharmacology and Toxicology
University of Arizona
Tucson, AZ 85724

Keywords: nanoparticle, locked nucleic acid, biosensor, single cell, tissue microenvironment

A. Supplementary Methods

Preparation of Nanoparticle-LNA complexes

Two types of nanoparticles with different shapes and coatings were used in the study. The spherical citrate coated gold nanoparticle (GNP) had a diameter of 10 nm in 0.1 mM PBS (Sigma-Aldrich, No. 752584). The gold nanorod (GNR) was 10 nm in diameter, 67 nm in length (Nanopartz, No. C12-10-1064), and was modified with mercaptoundecyltrimethylammonium bromide (MUTAB). The LNA probe was prepared at 100 nM in 1x Tris-EDTA buffer. The LNA probe was first denatured at 95°C for 5 minutes in a water bath and was allowed to cool down to 70°C over the course of 1 hour. The nanoparticle solution was then mixed with the LNA probe solution and incubated at 70°C for 30 minutes. The nanoparticle-LNA complexes were then cooled down to room temperature over the course of 2 hours before they were ready for the experiment.

Probe design

The target mRNA sequences were obtained from the NCBI GenBank Database. The secondary structures of the target mRNAs were determined using the Mfold web server to assist the design of the LNA probe^[1]. The sequence specificity of each LNA probe was analyzed by the NCBI Basic Local Alignment Search Tool (BLAST) database. The length of each LNA probe was 20 bases with alternating LNA and DNA monomers, which were optimized for the sensitivity and specificity of the assay^[2,3]. A fluorophore (6-FAM) was placed at the 5' end of the LNA probe for fluorescence detection. The LNA probes and corresponding synthetic targets were synthesized by Integrated DNA Technologies Inc. (IDT).

Nanoparticle uptake

Human Umbilical Vein Endothelial Cells (HUVECs) with a concentration of 5×10^4 cells per mL were seeded on 24 well tissue culture well plates. After culturing overnight to allow for cell attachment, GNP and GNR with a concentration of $12 \mu\text{g/mL}$ were added to the wells. To study GNP and GNR internalization kinetics, the cells were harvested at 3 h, 6 h, 9 h, 12 h, 18 h, 24 h, and 48 h. The cells were washed 3 times using 1x PBS to remove the GNP and GNR that were not internalized. The harvested cells were then counted using a hemocytometer (Hausser Scientific). The harvested cells with internalized gold nanoparticles were suspended in aqua regia digestion solution and lysed using a microwave digestion system (MARS-6, CEM Corporation, Matthew, NC). After digestion, the amount of gold in different samples were estimated using an inductively coupled plasma mass spectrometry (ICP-MS) system (7700x, Agilent Technologies, Santa Clara, CA).

To optimize the internalization of nanoparticles by cells, HUVECs were incubated with different concentrations of GNR and GNP ($3 \mu\text{g/mL}$, $6 \mu\text{g/mL}$, $12 \mu\text{g/mL}$, $24 \mu\text{g/mL}$ and $48 \mu\text{g/mL}$). After 12 hours of incubation, cells were harvested and counted. The internalized GNP and GNR were quantified using ICP-MS system. Figure S1a shows the amount of nanoparticles internalized into the cells at different incubation concentrations. It should be noted that the GNP and GNR could be detected as early as two hours of incubation. The nanoparticles internalized in endothelial cells were maximized and saturated after 24 hours (Figure S1b). The amount of nanoparticles generally increased with the incubation concentration. The difference in

internalization rates of GNR and GNP could be understood by the shape, size, and surface coating^[4, 5].

Cell viability

The cytotoxicity of GNR and GNP was characterized by observing the cell morphology and measuring the viability with a cell proliferation assay (Cell Counting Kit-8, CCK-8 assay). To evaluate the effects of nanoparticles on cells, HUVECs at a concentration of 1000 cells per mL were seeded in flat-bottom 96-well tissue culture plates and were incubated at 37°C and 5% CO₂ for 24 to 72 hours. After 12 hours of incubation for cell attachment and stabilization, different concentrations of nanoparticles were added and incubated with the cells for 48 hours. A microculture plate reader (BioRad) was used to measure the absorbance values of the samples at 450 nm. Figure S2a shows the cell viability after 48 hours incubation. The cell viability was normalized to the number of untreated cells, i.e., 100% cell viability. Both GNR and GNP addition caused low cytotoxicity. Over 90% cell viability was observed even when the GNR or GNP concentration was as high as 24 µg/mL. It should be noted that intracellular mRNA expression was detectable with as little as 2 µg/mL gold nanoparticles. The optimized protocol enabled the internalization of nanoparticle-LNA probes for single cell gene expression dynamics monitoring without significant effects on cell behavior and viability. Unless otherwise specified, the standard concentration of nanoparticles used in this study was 12 µg/mL. Furthermore, the GNR was less toxic than the GNP with the same mass of gold (Figure S2a). Since nanoparticles have a different surface to volume ratios, the effects of the nanoparticles on cell viability were also compared based on the surface area (Figure S2b). Similarly, the GNR was less toxic than

the GNP. The difference in cell viability may be primarily due to the different surface coatings for GNR and GNP, which plays important roles in nanoparticle cytotoxicity^[5, 6]. These results indicate that GNR has better biocompatibility compared to GNP for single cell gene expression analysis.

Absorbance of GNR and GNP

The absorbance spectra of the GNR and GNP were measured by UV-vis-NIR spectrophotometry (Figure S3). An absorption peak at 525 nm was observed for the GNP. Two absorption peaks at 525 nm and 950 nm were seen in the absorption spectrum of the GNR; the absorption peaks corresponded to the transverse and longitudinal plasmon resonance modes along the short and long axes of the GNR.

Tube formation assay

HUVECs with a density of 2×10^4 cells per mL were seeded on a 35 mm cell culture dish (Figure S4). When the cells reached 70-80% confluence, the GNR-LNA probes at 2×10^{11} particles per mL were incubated with HUVECs. After 8 hours, the cells were washed with $1 \times$ PBS 3 times and harvested. After internalization of GNR-LNA probes, cells were seeded on Matrigel-precoated glass bottom 24 well tissue culture plates at a seeding concentration of 2×10^4 cells per mL. *In vitro* capillary networks were self-organized on Matrigel after 3 hours of incubation. Single cell gene expression was then measured in the capillary networks. For the Dll4 experiments, HUVECs were treated with 10 μ M DAPT (Sigma-Aldrich, No. D5942) and 10 μ M

Jagged1 (GenScript, No. 188-204) to modulate the capillary formation process. A random, scrambled probe was used as a control.

B. Equilibrium analysis

The binding affinity and the free energy change (ΔG) play a critical role in the LNA probe design. In particular, the relative binding affinity directly determines the sensitivity and specificity of the biosensor. The binding dynamics of the double-stranded displacement probe has been previously analyzed^[2, 7, 8]. The competitive binding reactions of the nanoparticle-LNA assays can be described using equations 1 and 2.



In this model, $[L]$ is the concentration of fluorophore-labeled LNA probes, $[G]$ is the concentration of total available binding sites on nanoparticles, $[LG]$ is the concentration of nanoparticle-LNA complexes, $[T]$ is the concentration of target molecules, and $[LT]$ is the concentration of LNA-target complexes. **At equilibrium, the equilibrium constant can be determined by equations 3-4, where k_1 and k_2 are equilibrium constants of nanoparticle-LNA and LNA-target, respectively.**

$$k_1 = \frac{[LG]}{[L][G]} \quad (3)$$

$$k_2 = \frac{[LT]}{[L][T]} \quad (4)$$

To estimate the binding affinity of LNA probe and gold nanoparticles, the concentration of the free fluorophore probe can be determined by solving the equations without the target (equations

3, 5, 6, and 7)^[2, 7, 8]. Since each nanoparticle can bind to multiple LNA probes, the number of effective binding sites should be corrected based on the experimental concentration. The physical parameters, k_I and M , can be determined by fitting equation 8 with experimental data.

$$G_0 = ML_0 \quad (5)$$

$$L_0 = [L] + [LG] \quad (6)$$

$$G_0 = [G] + [LG] \quad (7)$$

$$[L] = \frac{k_1 \cdot (1-M) \cdot L_0 - 1 + \sqrt{[1 - k_1 \cdot (1-M) \cdot L_0] + 4 \cdot k_1 \cdot L_0}}{2 \cdot k_1} \quad (8)$$

Figures S5a and S5b show the fluorescence intensities of the probes with different LNA-nanoparticle ratios. The data were fitted with equation 8 to estimate the physical parameters. The results indicate that each GNR has approximately 80 effective binding sites and each GNP has 25 effective binding sites, which are in good agreement with the surface areas of the nanoparticles. The free energy changes of the binding reactions were estimated based on the equilibrium constants. The free energy changes, $\Delta G = -RT \cdot \ln(k_I)$, for GNR-LNA and GNP-LNA binding were -27.45 kcal/mol and -24.71 kcal/mol, with the equilibrium constants $k_{I(GNR)} = 1 \times 10^{20}$, and $k_{I(GNP)} = 1 \times 10^{18}$, respectively. These results indicate GNR has a stronger binding affinity with LNA compared to GNP. These free energy values are significantly lower than binding with a complementary nucleic acid sequence of 10 bases ($\Delta G = -14.94$ kcal/mol and $k_{I(10bases)} = 7.66 \times 10^{10}$), supporting the ability of the nanoparticle-LNA biosensor to prevent non-specific binding in the cells. The difference between the equilibrium constants of the nanoparticles could be a result of the surface coatings and shapes of the nanoparticles.

To optimize the sensing performance, the dynamic ranges of the biosensors were estimated based on experimental data and equilibrium analysis. Assuming that the number of binding sites is large compared to the number of LNA probes, the total concentrations of LNA, nanoparticles, and target, L_0 , T_0 , and G_0 , are described by equations 9-11.

$$L_0 = [L] + [LG] + [LT] \quad (9)$$

$$T_0 = [LT] + [T] \quad (10)$$

$$G_0 = [G] \quad (11)$$

Solving equations 3, 4, 9, 10 and 11, the target concentration $[T]$ and LNA-target complex concentration $[LT]$ can be estimated:

$$[T] = T_0 - [LT] = T_0 - \frac{k_2 T_0 [L]}{1+k_2 [L]} = \frac{T_0}{1+k_2 [L]} \quad (12)$$

$$[LT] = \frac{k_2 T_0 [L]}{1+k_2 [L]} \quad (13)$$

$$[L] = L_0 - k_1 \cdot [L] \cdot G_0 - \frac{k_2 \cdot T \cdot [L]}{1+k_2 \cdot [L]} \quad (14)$$

The concentration of LNA-target complex $[LT]$ can be calculated using equations 13-14. A titration experiment was performed using synthetic targets (Figure S6a-b). The biosensors have a dynamic range spanning across three orders of magnitude for target concentrations. Since k_1 has already been determined, k_2 can be extracted by fitting with the data. The free energy change and equilibrium constant for LNA-target binding were estimated to be -35.68 kcal/mol and 1×10^{26} . The values are in good agreement with the web-based oligo design software (IDT SciTool), which predicts $\Delta G = -34.45$ kcal/mol and $k_2 = 1.25 \times 10^{25}$. The binding affinity of LNA-target is therefore stronger than the binding affinity of LNA-GNR, allowing the target to displace the LNA probe from the nanoparticle thermodynamically.

Table S1. LNA probes and synthetic DNA targets used in this study

Name		Sequence (5'-3')	Fluorophore
β -actin (H)	Donor	+AG+GA+AG+GA+AG+GC+TG+GA+AG+AG	/56-FAM
	Target	CTCTTCCAGCCTTCCTTCCT	
Dll4 (H)	Donor	+AA+GG+GC+AG +TT+GG+AG+AG+GG+TT	/56-FAM
	Target	AACCCTCTCCA ACTGCCCTT	
β -actin (M)	Donor	+AG+TA+TT+AA+GG+CG+GA+AG+AT+TT	/56-FAM
	Target	AAATCTTCCGCCTTAATACT	
Dll4 (M)	Donor	+TG+GT+TC+TG+CA+CT+TT+GC+CA+CA	/56-FAM
	Target	TGTGGCAAAGTGCAGAACCA	
Random	Donor	+AC+GC+GA+CA+AG+CG+CA+CC+GA+TA	/56-FAM
	Target	TATCGGTGCGCTTGTCGCGT	

* H represents *homo sapiens*, and M represents *mus musculus*, + represents LNA monomer

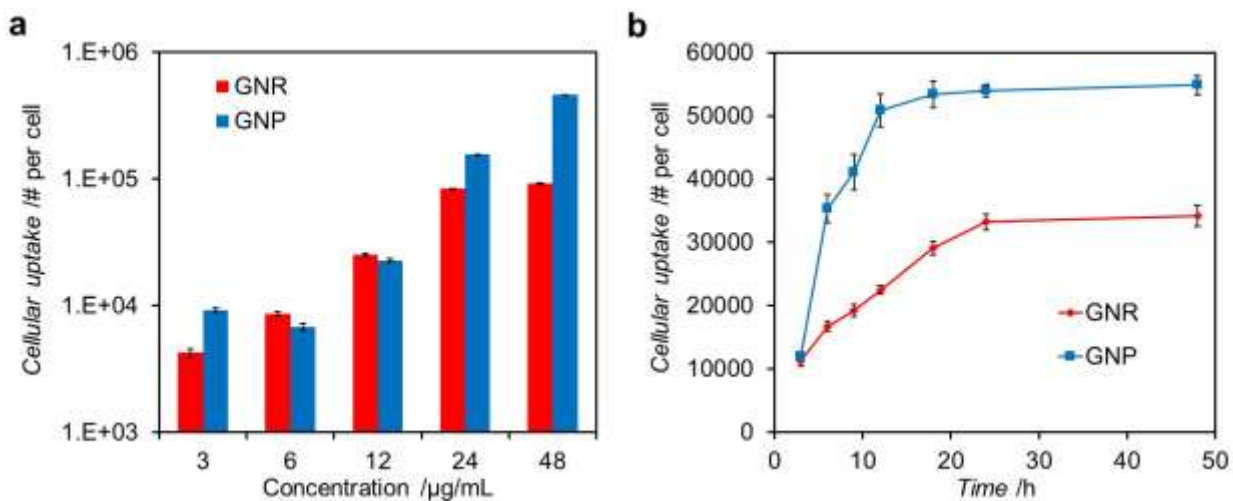


Figure S1. Optimization of GNP and GNR uptake. (a) Internalization of GNP and GNR with different concentrations. (b) Kinetics of nanoparticle internalization. The concentration of nanoparticles was 12 $\mu\text{g/mL}$. Data represent mean \pm s.e.m. (n=3).

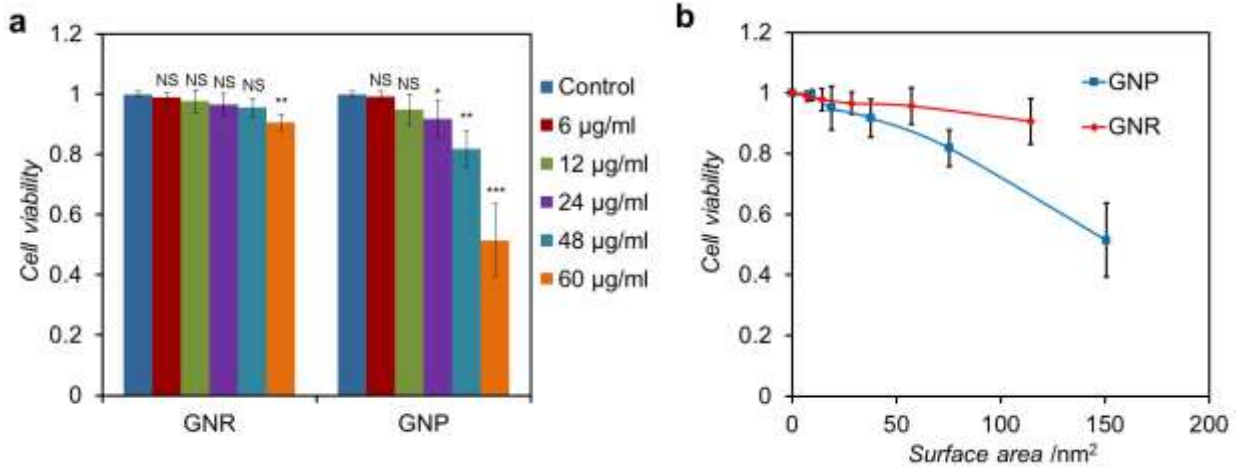


Figure S2. The effects of nanoparticles on cell viability. (a) The viability of HUVECs after incubation with different nanoparticle concentrations. (b) The effect of nanoparticles on cell viability estimated based on the surface area. Student's t-tests were performed to compare the data to control. *P < 0.05, **P < 0.01, ***P < 0.001. Data are expressed as mean \pm s.e.m. (n=5).

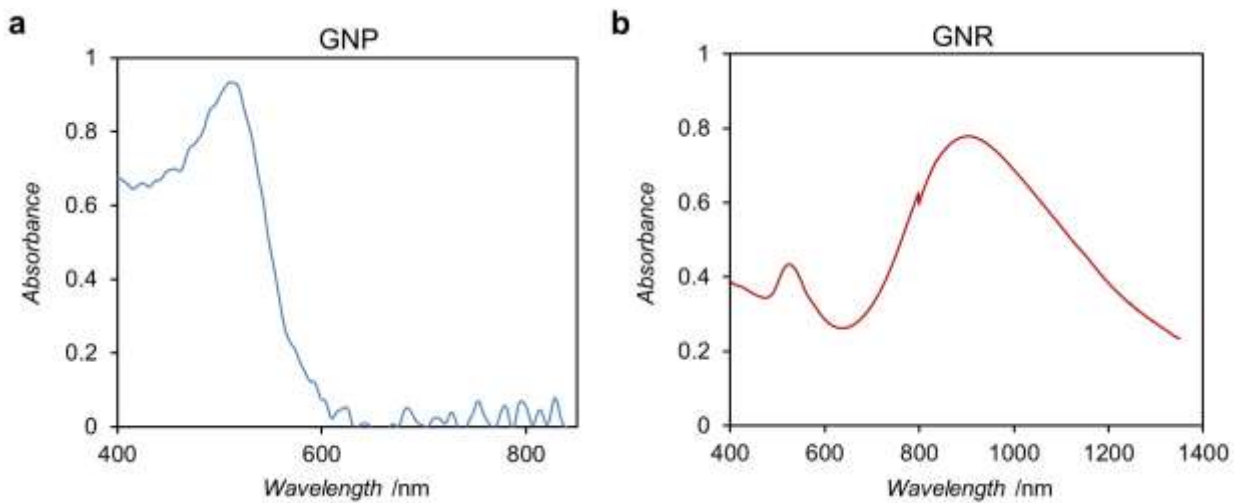


Figure S3. UV-vis-NIR absorption spectra of (a) GNP and (b) GNR.

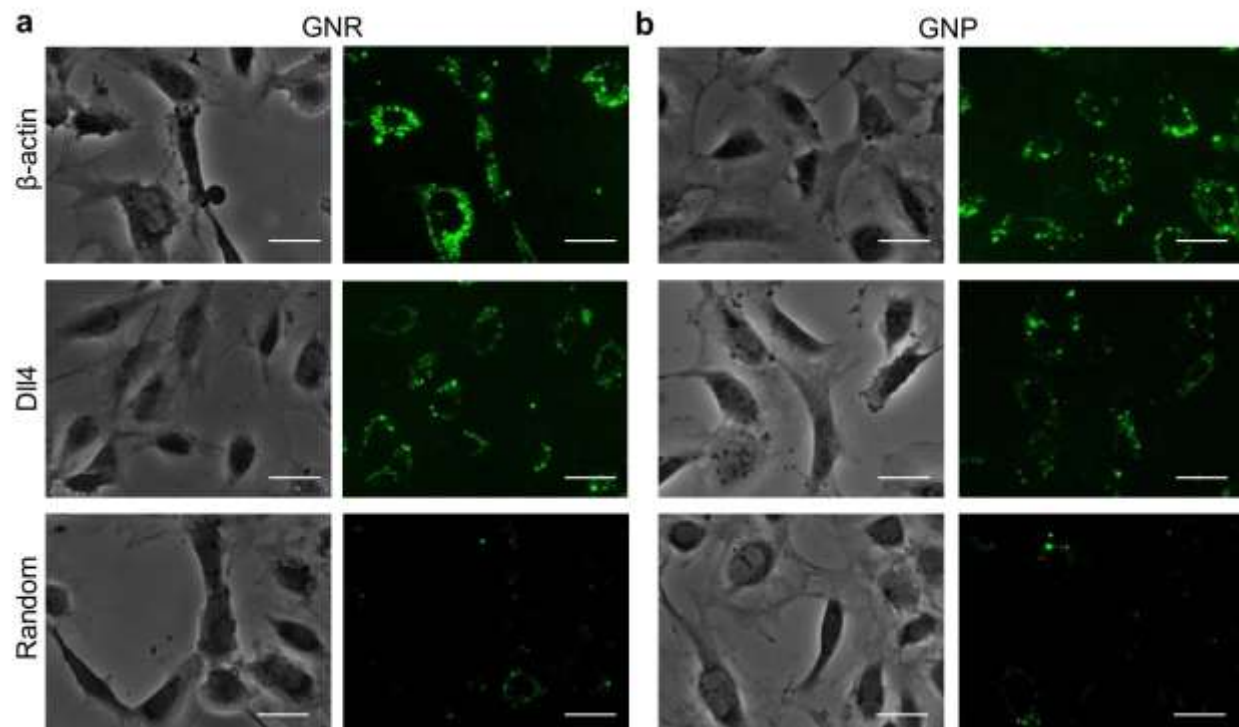


Figure S4. (a-b) Brightfield and fluorescence images of HUVEC with LNA probes targeting β -actin, Dll4, and random sequence control. The experiments were performed with (a) GNR and (b) GNP. Scale bars, 20 μ m.

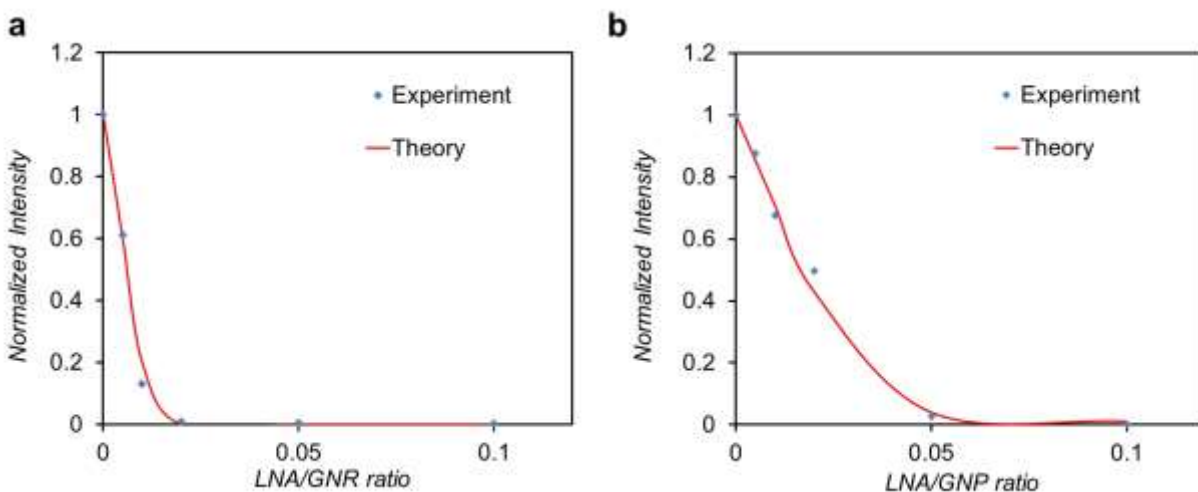


Figure S5. Calibration of the LNA-nanoparticle ratio for parameter estimation in the equilibrium analysis. (a-b) The equilibrium concentration of free fluorophore determined by equilibrium analysis and experiments. The values are normalized for comparison. The experiments were performed with (a) GNR and (b) GNP.

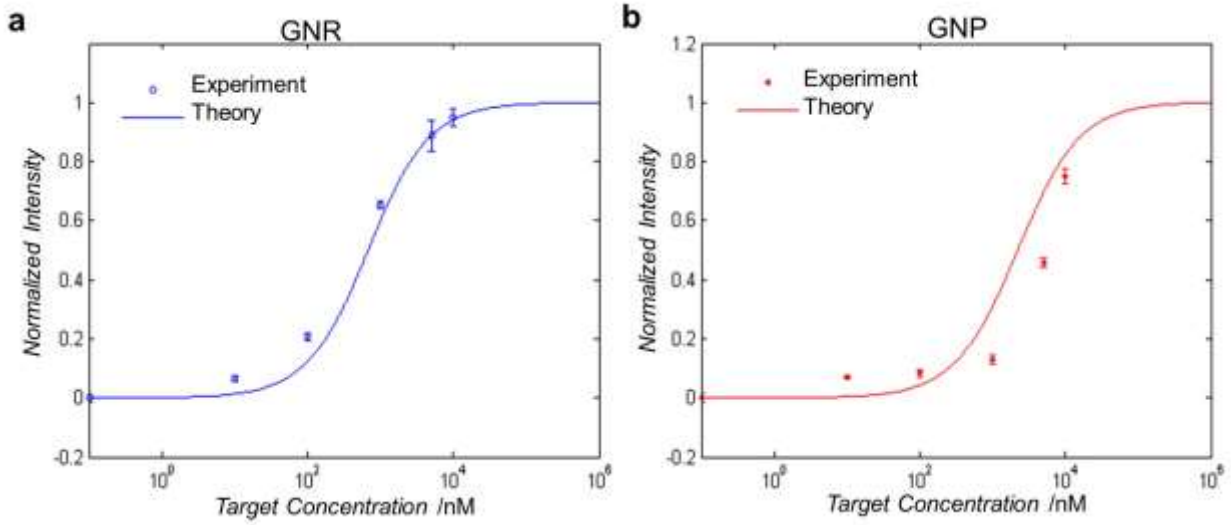


Figure S6. Calibration of the sensing performance with synthetic targets. The experiments were performed with (a) GNR and (b) GNP.

Reference

- [1] M. Zuker, *Nucleic Acids Research* 2003, 31, 3406.
- [2] R. Riahi, Z. Dean, T. H. Wu, M. A. Teitell, P. Y. Chiou, D. D. Zhang, P. K. Wong, *Analyst* 2013, 138, 4777.
- [3] R. Riahi, S. Wang, M. Long, N. Li, P. Y. Chiou, D. D. Zhang, P. K. Wong, *Acs Nano* 2014, 8, 3597.
- [4] B. D. Chithrani, A. A. Ghazani, W. C. W. Chan, *Nano Letters* 2006, 6, 662.
- [5] C. Freese, C. Uboldi, M. I. Gibson, R. E. Unger, B. B. Weksler, I. A. Romero, P. O. Couraud, C. J. Kirkpatrick, *Part Fibre Toxicol* 2012, 9, 23.
- [6] E. E. Connor, J. Mwamuka, A. Gole, C. J. Murphy, M. D. Wyatt, *Small* 2005, 1, 325.
- [7] V. Gidwani, R. Riahi, D. D. Zhang, P. K. Wong, *Analyst* 2009, 134, 1675.
- [8] D. Meserve, Z. Wang, D. D. Zhang, P. K. Wong, *Analyst* 2008, 133, 1013.